MATERIALS AND PRODUCT ENGINEERING
Chinese Journal of Chemical Engineering, **21**(2) 113—120 (2013)
DOI: 10.1016/S1004-9541(13)60448-6

ZrO_2/PMMA Nanocomposites: Preparation and Its Dispersion in Polymer Matrix*

FAN Fangqiang (范方强)**, XIA Zhengbin** (夏正斌)**, LI Qingying** (李清英)**, LI Zhong** (李忠) **and CHEN Huanqin** (陈焕钦)
School of Chemistry and Chemical Engineering, South China University of Technology, Guangzhou 510640, China

Abstract ZrO_2/PMMA nanocomposite particles are synthesized through an *in-situ* free radical emulsion polymerization based on the silane coupling agent (Z-6030) modified ZrO_2 nanoparticles, and the morphology, size and its distribution of nanocomposite particles are investigated. Scanning electron microscopy (SEM) images demonstrate that the methyl methacrylate (MMA) feeding rate has a significant effect on the particle size and morphology. When the MMA feeding rate decreases from 0.42 ml·min^{-1} to 0.08 ml·min^{-1}, large particles (about 200–550 nm) will not form, and the size distribution become narrow (36–54 nm). The average nanocomposite particles size increases from 34 nm to 55 nm, as the MMA/ZrO_2 nanoparticles mass ratio increased from 4 : 1 to 16 : 1. Regular spherical ZrO_2/PMMA nanocomposite particles are synthesized when the emulsifier OP-10 concentration is 2 mg·ml^{-1}. The nanocomposite particles could be mixed with VAc-VeoVa10 polymer matrix just by magnetic stirring to prepare the ZrO_2/PMMA/VAc-VeoVa10 hybrid coatings. SEM and atomic force microscopy (AFM) photos reveal that the distribution of the ZrO_2/PMMA nanocomposite particles in the VAc-VeoVa10 polymer matrix is homogenous and stable. Here, the grafted-PMMA polymer on ZrO_2 nanoparticles plays as a bridge which effectively connects the ZrO_2 nanoparticles and the VAc-VeoVa10 polymer matrix with improved comparability. In consequence, the hybrid coating with good dispersion stability is obtained.
Keywords ZrO_2 nanoparticles, core-shell structure, monomer feeding rate, dispersion stability

1 INTRODUCTION

Inorganic/organic nanocomposites are generally organic polymer composites with inorganic nanoscales building blocks, and combine the advantageous properties of inorganic materials (*e.g.*, rigidity, thermal stability) with that of organic materials (*e.g.*, flexibility, dielectric, ductility, and processability) [1]. Compared with micrometer-sized composites, the polymer nanocomposites exhibit new and improved properties, *e.g.*, dispersion stability, mechanical property, thermal stability and flame resistance [2–6], due to their nanometer phase dimensions. It has attracted great attentions world widely from both academic and industrial points of view, and shows potential in various applications, such as cosmetics, inks, and paints [2, 7–9].

The dispersion of nanometer-sized inorganic particles (hereafter nanoparticles) into the polymer matrix has a significant effect on the properties of nanocomposites. In general, two strategies have been employed for the fabrication of nanocomposites to meet the needs of the end user application [10]. The first is the simple and versatile physical method, including melt blending, high-energy ball milling and ultrasonic treatment, *etc*. In this case, the driving forces between nanoparticles and polymer matrix are van der Wall's forces and electrostatic interactions, *etc*. However, the physical method may not be efficient in dispersing nanoparticles homogenously in polymer matrix, because high surface energy of nanoparticles is prone to induce the formation of nanoparticles aggregation. Besides, phase separation often takes place owing to the great differences in the properties of polymer and inorganic materials [11]. The second is the chemical method, often used for preparing the inorganic core and polymer shell structure nanocomposites, by *in-situ* polymerization of monomers in the presence of inorganic nanoparticles. In this case, two techniques, the so-called "grafting to" [3, 4] and "grafting from" [12] methods are used to chemically modify the inorganic nanoparticles surface with polymer. The grafted-polymer increases the compatibility of inorganic nanoparticles and polymer matrix, enhances the dispersion stability of inorganic nanoparticles in nanometer dimensions in polymer matrix, and decreases the phase separation at a great extent. However, a large-scale up of this processing technique is still a challenge.

Zirconia has been largely used because of their chemical and physical properties such as excellent refractoriness, chemical resistance, good mechanical strength, low thermal conductivity at high temperature and good thermal stability [13–16]. Several methods have been developed to synthesize ZrO_2/polymer nanocomposite particles in the past decades. Pu *et al*. [17] synthesized ZrO_2/polymer nanocomposites by inductively coupled plasma polymerization. Transparent polymethyl methacrylate (PMMA)/SiO_2/ZrO_2 nanocomposites with excellent thermal properties were prepared using a non-hydrolytic sol-gel process [18]. Dubois *et al*. [19] reported that zirconia nanoparticles could be encapsulated in polyethylene *via* a polymerization compounding method by using a Ziegler-Natta

Received 2011-10-25, accepted 2012-05-24.
* Supported by Production, Teaching & Research Combination Project for Universities in Guangdong Province (cgzhzd0904), Department of Education of Guangdong Province, China.
** To whom correspondence should be addressed. E-mail: cezhbxia@scut.edu.cn

catalyst. In recent years, it was found that ZrO_2 nanoparticles could be modified with 2-acetoacetoxyethyl methacrylate (AAEM). Sayılkan *et al*. [20] synthesized ZrO_2/PAAEM nanocomposites for optical purposes by hydrothermal method. Wang *et al*. [21] utilized sol-gel method and emulsifier-free emulsion polymerization to prepare ZrO_2/PAAEM/polystyrene (PS) nanocomposites, and the thermal-gravimetry analyzer (TGA) results indicated that the ZrO_2 nanoparticles had significantly improved the thermal stability of PS. However, to the best of our knowledge, the encapsulation of ZrO_2 nanoparticles by using methyl methacrylate (MMA) as monomer has not been published in the literature.

In this paper, ZrO_2/PMMA nanocomposite particles are prepared by *in-situ* polymerization of MMA in the presence of ZrO_2 nanoparticles which are beforehand modified by the silane coupling agent γ-methacryloxypropyltrimethoxysilane (Z-6030). Then, the ZrO_2/PMMA nanocomposites are mixed into VAc-VeoVa10 polymer matrix, to prepare the water-based hybrid coatings material. The ZrO_2 nanoparticles encapsulation process and the mixing process of ZrO_2/PMMA nanocomposites with polymer matrix are separated. Firstly, the effect of several factors on the size and morphology of nanocomposites are investigated and characterized by using various advanced techniques. Then, the dispersion and the morphology of the hybrid coatings are investigated by scanning electron microscopy (SEM) and atomic force microscopy (AFM).

2 EXPERIMENTAL

2.1 Materials

Methyl methacrylate (MMA) was commercial product and was used without further purification. γ-methacryloxypropyltrimethoxysilane (Z-6030) was provided by Dow Corning Corporation. Zirconia powder (average diameter 30 nm) was purchased from Huizhou Dagite Metal Materials Co., Ltd. VAc-VeoVa10 polymer matrix was an aqueous copolymer dispersion based on vinyl acetate and vinyl ester of versatic acid (average diameter 300 nm, solid content 50%) and was purchased from Clariant Chemical (China) Co., Ltd. Absolute ethanol and isobutanol, analytical grade, were supplied by Guangzhou Chemical Reagent Co. 25%–28% ammonia, nonyl phenyl polyoxyethylene ether-10 (OP-10), sodium bicarbonate ($NaHCO_3$) and potassium persulfate (KPS) were used as received. Dispersant agent BYK-375 (reactive silicone surface additive) was provided by BYK Additives & Instruments (Germany). Deionized water was applied for the polymerization process.

2.2 Modification of nano-ZrO_2 by Z-6030

Nano-ZrO_2 surface was modified with Z-6030. Firstly, 5 g ZrO_2 powder was dispersed into 120 ml absolute ethanol with the aid of ultrasound bath (ultrasonic power 200 W) for 2 h. Z-6030 [3% (by mass) relative to ZrO_2] was added into an ethanol/water solution (ethanol/water = 19/1), then 2 $mol \cdot L^{-1}$ hydrochloric acid was dropped in until pH = 3. After hydrolysis for 1 h at room temperature under vigorously magnetic agitation, the solution was poured into a 500 ml three necked round bottomed glass reactor, which was equipped with a reflux condenser, a mechanical stirrer, and a thermograph, mixed with the dispersion of ZrO_2 nanoparticles ethanol solution. Then, the reactor was heated up to 50 °C, and the grafting reaction continued for 5 h with agitation at 200 $r \cdot min^{-1}$. After the reaction finished, the suspension was purified by washing with absolute ethanol and three cycles of centrifugation/re-dispersion (7000 $r \cdot min^{-1}$, 15 min). Z-6030 monomer in excess and oligomer resulted from homopolymerization of Z-6030 were entirely removed from the precipitate. The resulted precipitate was dried in vacuum at 100 °C for 24 h. Finally, 4.6 g nano-ZrO_2 modified by Z-6030 was obtained.

2.3 Preparation of ZrO_2/PMMA nanocomposites

Monodisperse core/shell polymer nanocomposites were synthesized by free radical emulsion polymerization. First, the modified nano-ZrO_2 was redispersed in aqueous solution by the Guyot method [22, 23]. In a typical experiment, 0.8 g of modified nano-ZrO_2 dispersed into 100 ml water, in which 0.4% isobutanol was added as a co-dispersion agent, 25%–28% ammonia was added in dropwise until pH = 9–10. After ultrasonicated for 1 h, the dispersion was transferred into a four necked round bottomed glass reactor with a reflux condenser, a mechanical stirrer, a thermograph, and a dropping tube. An amount of OP-10 was added as emulsifier. Then, the solution was stirred at the rate of 200 $r \cdot min^{-1}$ for 12 h, in order to absorb the emulsifier on the hydrophobic surface of modified nano-ZrO_2 sufficiently. A micelle-like structure with hydrophobic group inwards and hydrophilic group outwards was formed, inside which the free radical emulsion polymerization proceeded. After that, 0.3 g $NaHCO_3$ as buffer agent and 0.2 g KPS as initiator were added into the reactor. MMA was fed dropwisely in a variable rate, and the polymerization proceeded at 75 °C for 6 h. Then lower the temperature in the reactor to below 50 °C, and the emulsion of core/shell nanocomposites was obtained. The experimental formulations for preparation of ZrO_2/PMMA nanocomposites were listed in Table 1.

2.4 Preparation of ZrO_2/PMMA/VAc-VeoVa10 hybrid coatings

The hybrid coatings were prepared as follows: firstly, the ZrO_2/PMMA nanocomposite particles were separated by centrifugation/re-dispersion in deionized water (3 times, 7000 $r \cdot min^{-1}$, 20 min), in order to remove

Table 1 Experimental formulations for synthesis ZrO_2/PMMA nanocomposites

Sample number	Core material	Monomer feeding rate /ml·min^{-1}	Monomer/ZrO_2 mass ratio	Emulsifier (OP-10) concentration /mg·ml^{-1}
1	ZrO_2/Z-6030	0.42	16∶1	2
2	ZrO_2/Z-6030	0.21	16∶1	2
3	ZrO_2/Z-6030	0.13	16∶1	2
4	ZrO_2/Z-6030	0.08	16∶1	2
5	ZrO_2/Z-6030	0.13	8∶1	2
6	ZrO_2/Z-6030	0.13	4∶1	2
7	ZrO_2/Z-6030	0.08	16∶1	1
8	ZrO_2/Z-6030	0.08	16∶1	0.5
9	ZrO_2	0.13	16∶1	2

the neat PMMA particles. Then, 1% (mass percentage based on polymer matrix) of the ZrO_2/PMMA nanocomposite particles (sample 3) were mixed into VAc-VeoVa10 polymer matrix, and the hybrid coatings was obtained just by using magnetic stirrer agitated for 30 min. Reference samples were prepared by directly adding ZrO_2 nanoparticles into VAc-VeoVa10 polymer matrix and using magnetic stirrer agitated for 30 min, or prepared by first using ultrasonicated ZrO_2 nanoparticles with the wetting dispersant BYK-375 for 1 h, then mixed with VAc-VeoVa10 polymer matrix and using high-energy ball miller milled for 30 min. The coating films were prepared by pouring the hybrid coatings on watch glass and drying at ambient temperature. Fig. 1 is a sketch of preparation procedure of the hybrid coatings.

2.5 Characterization

Fourier transform infrared (FTIR) spectroscopy were measured in the wave number range from 4000 to 400 cm^{-1} at a resolution of 4 cm^{-1} using a Perkin-Elmer Spectnlm2000 to determine the chemical structure of

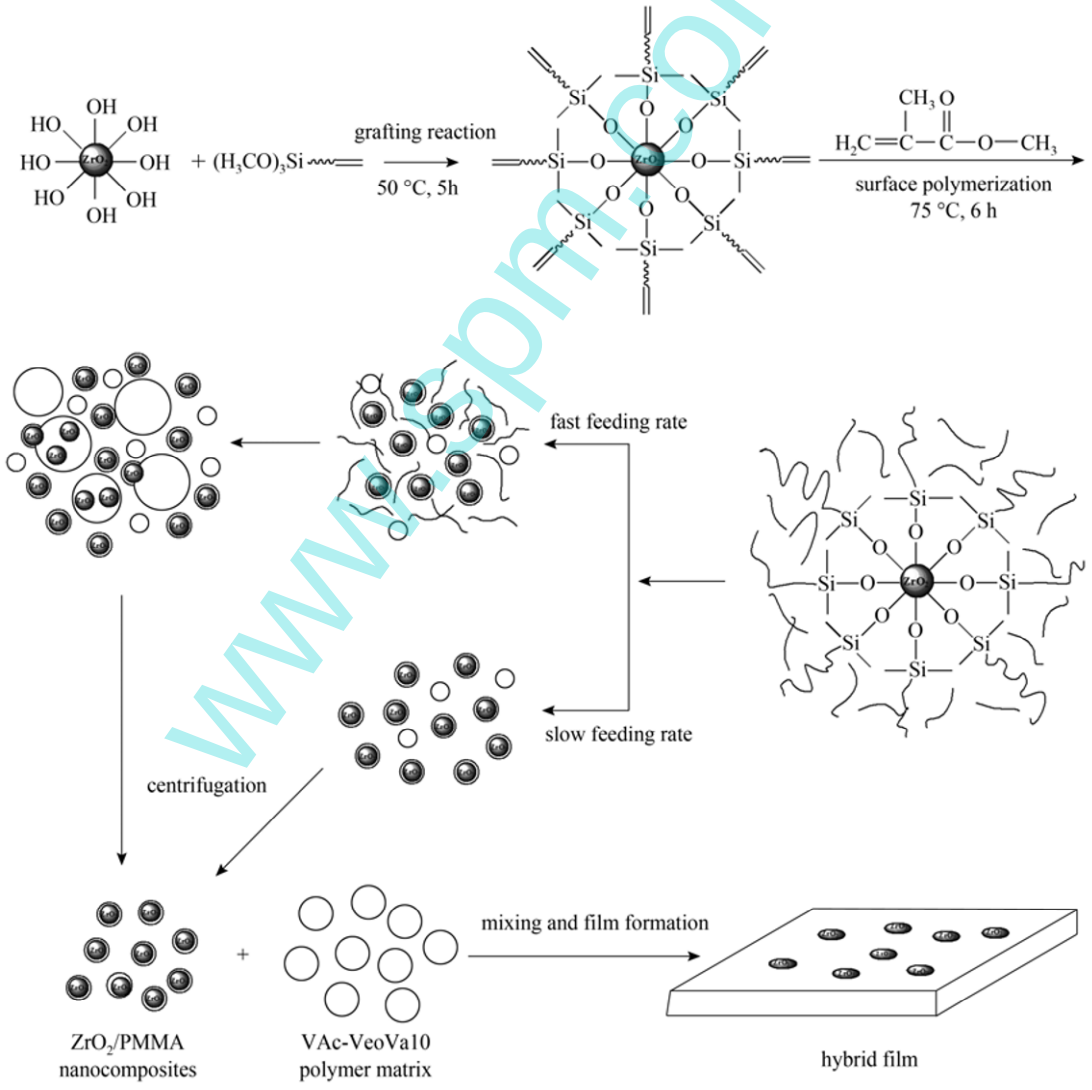

Figure 1 Preparation of ZrO_2/PMMA nanocomposites and formation of ZrO_2/PMMA/VAc-VeoVa10 hybrid film

ZrO_2, Z-6030 modified ZrO_2 and the ZrO_2/ PMMA after emulsion polymerization. The morphology of the synthesized particles were observed using field-emission scanning electron microscopy (FE-SEM, LEO1530VP, Zeiss Co., Germany) with 5.0 kV accelerating voltage, and transmission electron microscopy (TEM, H-7650, Hitachi Co., Japan) at 80 kV accelerating voltage. The SEM samples were prepared by placing a drop of aqueous dispersions of the particles (before centrifugation) onto glass sheets, and calibrating with a glass rod, dried at room temperature. The sample was sputter-coated with gold prior to observation. The TEM samples were prepared by placing a diluted drop of aqueous dispersion of the particles (which were after three times centrifugation/ re-dispersion) onto Cu grids supported with carbon film, then dried at room temperature. The surface morphology of hybrid coatings films were studied by a scanning probe microscopy (cspm-3000, Benyuan Nano Co., China), the films were prepared by placing a drop of hybrid coatings on glass disc and spinning on a rotary film machine, dried at 50 °C in oven.

3 RESULTS AND DISCUSSION

3.1 Z-6030 modified ZrO_2 nanoparticles

The original diameter of ZrO_2 nanoparticle is about 30 nm. Fig. 2 is the SEM micrograph of silane coupling agent Z-6030 grafted ZrO_2 nanoparticles. It demonstrates that the variation of size between ZrO_2 nanoparticles and surface grafted ZrO_2 nanoparticles is not obvious. This grafted ZrO_2 nanoparticles is used as core material and MMA is used as shell material in the following free radical emulsion polymerization.

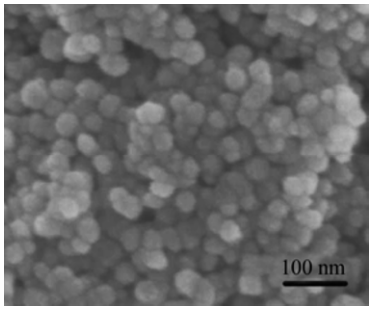

Figure 2 SEM image of Z-6030 grafted ZrO_2 nanoparticles

3.2 FTIR analysis

The chemical structures of ZrO_2 nanoparticles, Z-6030 modified ZrO_2 and the ZrO_2/PMMA nanocomposite particles are characterized by FTIR spectroscopy, and the results are shown in Fig. 3. In spectrum a, the absorption peaks around 3434 cm^{-1} are associated with stretching vibrations of —OH on the surface of ZrO_2 nanoparticles, while the absorption peaks at 740 cm^{-1} and 530 cm^{-1} are attributed to Zr—O stretching vibrations. The characteristic peaks of the stretching vibration bands of the Si—O—C, C═O and C—H bonds at 1174, 1732 and 2953 cm^{-1} are observed in spectrum b, respectively, and the absorption peak at 1632 cm^{-1} is attributed to C═C group in the Z-6030 molecular. These elucidate that the silane coupling agent Z-6030 is grafted onto the surface of ZrO_2 nanoparticles. In curve c, the characteristic stretching vibration peaks of —CH_3 and —CH_2— group exhibit at 2951 cm^{-1} and 2996 cm^{-1}, as well as the distortion vibration peak of —CH_2— group appear at 1448 cm^{-1} after the free

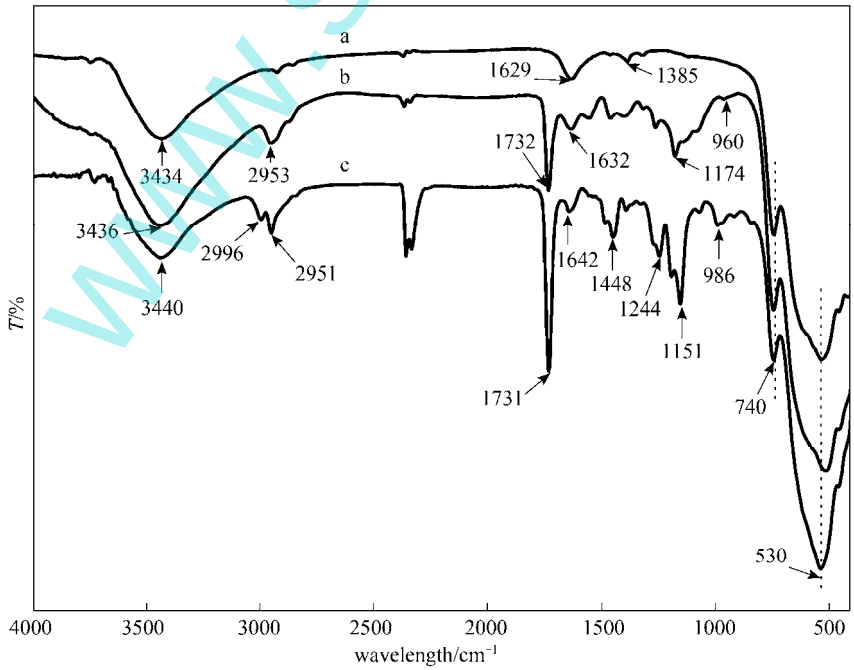

Figure 3 FTIR spectroscopy of (a) ZrO_2, (b) Z-6030 modified ZrO_2, and (c) ZrO_2/PMMA nanocomposite particles

radical polymerization of MMA on the grafted ZrO_2 surface. The absorption peak at 1731 cm^{-1} belong to C═O (carbonyl) asymmetric stretching vibration. The stretching vibration peaks of C—O—C at 1244 and 1151 cm^{-1} are attributed to PMMA. It is noted that the absorption peak of C═C group transfers from 1632 cm^{-1} to 1642 cm^{-1}, and the peak height decreases significantly in comparison with that of the Z-6030 modified ZrO_2 (compared the C═C/C═O in each curve), which indicates that the C═C group of the Z-6030 modified ZrO_2 is participated in the free radical polymerization of MMA monomer and the inorganic (core)/organic (shell) structure nanocomposites are synthesized.

3.3 Preparation of ZrO_2/PMMA nanocomposite particles

3.3.1 *Effect of MMA feeding rate*

The MMA free radical emulsion polymerization is taken place on the surface of Z-6030 grafted ZrO_2 nanoparticles. Fig. 4 is a series of SEM micrographs of ZrO_2 (core)/PMMA (shell) microspheres which are prepared at different MMA feeding rate. In Fig. 4 (a) or 4 (b), we find that two kinds of particles, different in size [370–550 nm, 74–185 nm in Fig. 4 (a), and 220–370 nm, 40–110 nm in Fig. 4 (b)], are prepared at the MMA feeding rate of 0.42 ml·min^{-1} and 0.21 ml·min^{-1}, respectively. The raspberry-like and dumb-bell-like microspheres are apparently showed in Fig. 4 (a). When the feeding rate decreases to 0.13 ml·min^{-1}, the average size of the composite particles is about 55 nm. The average particle size decreases to 45 nm when the monomer feeding rate is 0.08 ml·min^{-1}. With the feeding rate decreases from 0.42 ml·min^{-1} to 0.08 ml·min^{-1}, the larger particle (370–550 nm) disappear gradually and the particle size distribution become narrow (36–54 nm).

It is clearly shown that the monomer feeding rate has a pronounced effect on the composite particles size and distribution. When the monomer feeding rate is too fast (*e.g.* 0.42 ml·min^{-1}), the monomer of MMA tends to homopolymerization instead of copolymerization with the Z-6030 modified ZrO_2 nanoparticles. The chain of the homopolymer and oligomer adsorbs onto two or more ZrO_2 nanoparticles, and/or winds with the copolymer chain of ZrO_2 surface. Particle combination occurs between the homopolymer, oligomer and ZrO_2/PMMA composite particles, because of the bridging effect of this particle-polymer with each other [24–26]. On the contrary, the slower feeding rate is preferable for the copolymerization of the C═C bond on the Z-6030 modified ZrO_2 surface with the MMA monomer, reducing the MMA homopolymerization, and obtaining the ZrO_2/PMMA nanocomposites with a uniform particle size.

3.3.2 *Effect of monomer/ZrO_2 mass ratio*

The SEM photos of nanocomposite particles with different monomer/ZrO_2 nanoparticles mass ratio are shown in Fig. 5. It indicates that there is a positive correlation between the particle size and the monomer/ZrO_2 nanoparticles mass ratio in the range of this work. The average particle size is 34 nm when the monomer/ZrO_2 nanoparticles mass ratio is 4∶1 [Fig. 5 (a)]. As the ratio increases to 8∶1, the particles size increase

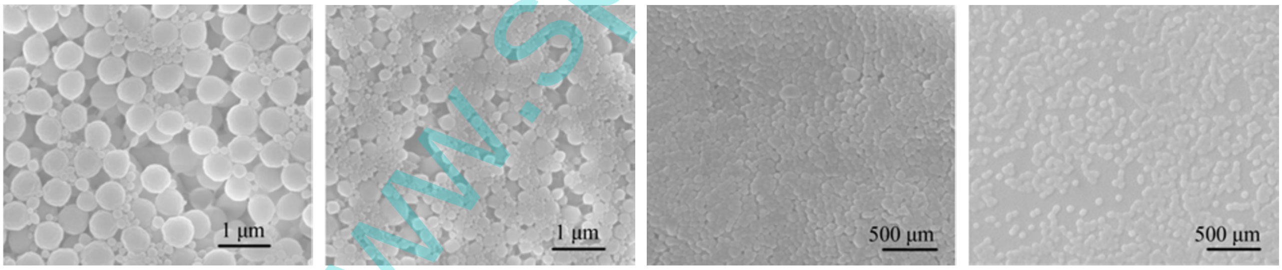

(a) 0.42 ml·min^{-1} (b) 0.21 ml·min^{-1} (c) 0.13 ml·min^{-1} (d) 0.08 ml·min^{-1}

Figure 4 SEM images of ZrO_2/PMMA nanocomposite particles at different MMA adding rate

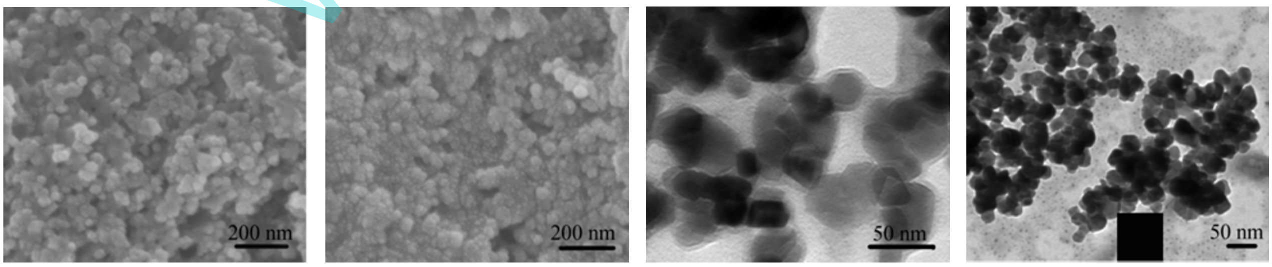

(a) (b) (c) (d)

Figure 5 Micrographs of ZrO_2/PMMA nanocomposites
[SEM graphs in monomer/ZrO_2 mass ratio (a) 8∶1 and (b) 4∶1; TEM graphs (c) monomer/ZrO_2 = 8 and (d) ZrO_2/PMMA without Z-6030 modified]

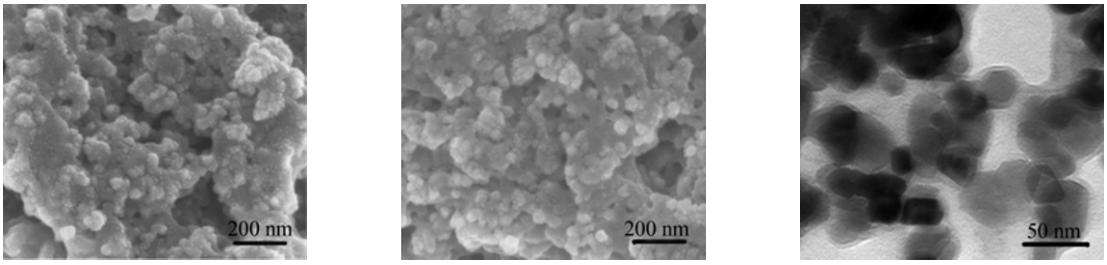

(a) (b) (c)

Figure 6 Micrographs of ZrO_2/PMMA nanocomposites in different emulsifier concentration [SEM graph (a) 0.5 mg·ml^{-1} and (b) 1 mg·ml^{-1}; TEM graph (c) 0.5 mg·ml^{-1}]

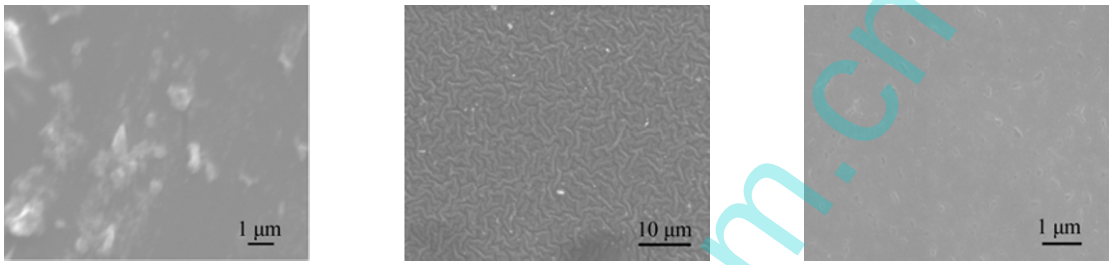

(a) ZrO_2 directly added (b) ZrO_2 /BYK-375 and ball milling (c) ZrO_2/PMMA

Figure 7 SEM photos of ZrO_2/VAc-VeoVa10 hybrid film

to 42 nm [Fig. 5 (b)], and the shell thickness is about 6 nm shown in the TEM image in Fig. 5(c). The average particle diameter is 55 nm when the monomer/ZrO_2 nanoparticles mass ratio increases to 16∶1, and a small amount of particles with the diameter of 200 nm are synthesized [Fig. 4 (c)]. The TEM graph in Fig. 5 (d) demonstrates that no grafting polymerization has taken place on the surface of ZrO_2 nanoparticles not modified by Z-6030. The results illustrate that the C═C bonds on the ZrO_2 nanoparticle surface, introduced by Z-6030 modification, determine the site of MMA polymerization. With the increase of the MMA concentration, the adsorbed surfactant on surface of the core material is depleted by the excessive monomer, and the polymerization is mostly occurred in term of self-nucleation [27].

3.3.3 *Effect of the emulsifier concentration*

The emulsifier absorbs on the modified ZrO_2 particle surface and the hydrophilic group heads to water to form a hydrophobic microreactor, and the MMA polymerization takes place in this micelle-like structure. A set of experiment are carried out with the fixed amount of MMA and ZrO_2 but variable concentration of emulsifier, and the final particles are characterized by SEM as shown in Fig. 6. It is seen that the average particle size of the ZrO_2/PMMA nanocomposites slightly decreases from 47 nm to 40 nm as the emulsifier concentration increases from 0.5 mg·ml^{-1} to 1 mg·ml^{-1}. At higher emulsifier concentration, the number of neat PMMA particles increases because the homopolymerization of MMA in micelle is easier than graft copolymerization with the modified ZrO_2 nanoparticles. However, the morphology of the composites particle becomes spherical at the concentration of 2 mg·ml^{-1} [Fig. 4 (d)]. The core-shell structure is shown in the TEM image in Fig. 6 (c), in which the emulsifier concentration is 0.5 mg·ml^{-1}.

3.4 The morphology of hybrid coatings film

The distribution of ZrO_2/PMMA nanocomposite particles in VAc-VeoVa10 polymer matrix are investigated by SEM, and the results are shown in Fig. 7. First, the severe aggregation of particles is observed when the ZrO_2 nanoparticles are mixed with VAc-VeoVa10 polymer matrix directly by magnetic stirrer agitation [Fig. 7 (a)]. The ZrO_2 nanoparticles accumulate on the surface of polymer film, which demonstrates that phase separation occurs during film formation. After modified by wetting dispersant and treated with high-energy ball miller, the ZrO_2 nanoparticles are relatively easy to disperse into the polymer matrix [Fig. 7 (b)], but the aggregation still occurs, and the aggregate size is larger than 310 nm. These results reveal that the particle aggregation can not eliminate entirely by a physical method. Fig. 7 (c) is the SEM photo of hybrid coatings film made of ZrO_2/PMMA nanocomposite particles and VAc-VeoVa10 polymer emulsion, suggesting that the ZrO_2/PMMA nanoparticles are homogeneously distributed in VAc-VeoVa10 polymer matrix. The grafted-PMMA polymer shell promotes the hydrophobicity of ZrO_2 nanoparticles, and behaves as a bridge to reduce the density mismatch between ZrO_2 nanoparticles and VAc-VeoVa10 polymer matrix. So, the method of preparing ZrO_2/PMMA nanocomposite particles not only makes the ZrO_2 nanoparticles

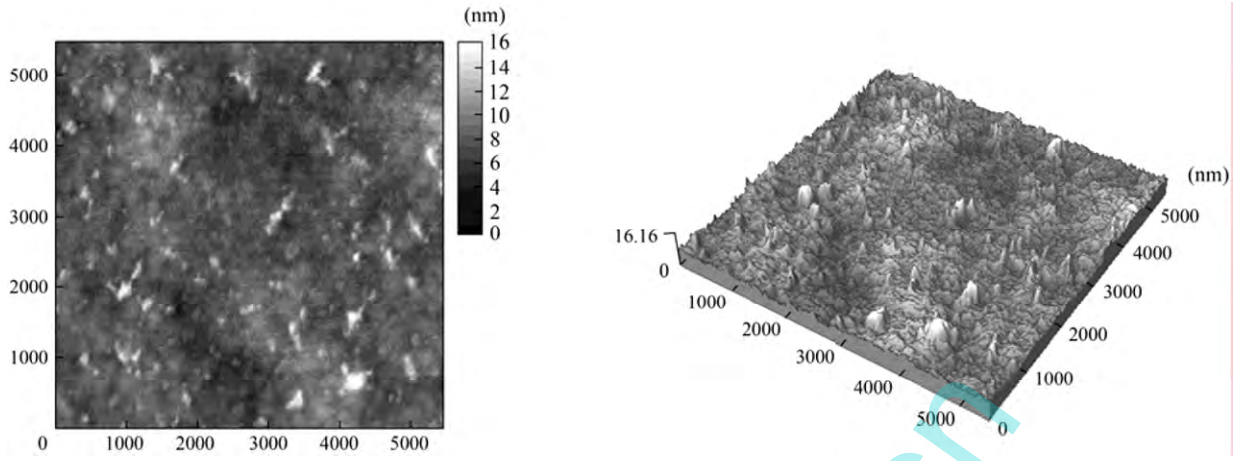

(a) Two-dimensional (b) Three-dimensional

Figure 8 AFM images of ZrO_2/PMMA/VAc-VeoVa10 hybrid film

homogenously dispersed in the polymer matrix, but also increases the compatibility between these two components. Therefore, based on the ZrO_2/PMMA nanoparticles, the hybrid coating with good dispersion stability is obtained.

Figure 8 is the AFM topographic images of the ZrO_2/PMMA/VAc-VeoVa10 hybrid coatings film with 1% (by mass) ZrO_2 nanoparticles. Fig. 8 (a) reveals that the ZrO_2 nanoparticles are uniformly distributed in the polymer matrix, which is in accordance with the SEM micrograph in Fig. 7. The closer observation of this image discovers that the ZrO_2 nanocomposite particles size is in the range of 40−100 nm, but large aggregates with the size range of 200−300 nm are also found in Fig. 8 (a). The average roughness (R_a) and root mean square roughness (R_q) of the hybrid coatings film is 1.09 nm and 1.47 nm, respectively. These results indicate that the hybrid film based on the ZrO_2/PMMA nanocomposites is quite smooth.

4 CONCLUSIONS

In this paper, a two-step method is used to prepare ZrO_2/PMMA/VAc-VeoVa10 hybrid coatings. In the first step, ZrO_2/PMMA nanocomposite particles are prepared through *in-situ* free radical emulsion polymerization of MMA on the surface of silane coupling agent modified ZrO_2 nanoparticles, and the effect of several factors on the nanoparticles size and morphology are investigated. The monomer feeding rate has marked effect on the size distribution and morphology of nanocomposite particles. SEM micrographs demonstrate that large particles (370−550 nm) disappear gradually as the monomer feeding rate decreases from 0.42 ml·min^{-1} to 0.08 ml·min^{-1}, and the particle size distribution become narrower (36−54 nm). The average diameter of nanocomposite particles increase from 34 nm to 55 nm as the monomer/ZrO_2 nanoparticles mass ratio increases from 4∶1 to 16∶1. The stability of the emulsion polymerization system is increased as the emulsifier increasing from 0.05 mg·ml^{-1} to 2 mg·ml^{-1}. Meanwhile, regular spherical composite particles are obtained at the emulsifier concentration of 2 mg·ml^{-1}. In the second step, the prepared ZrO_2/PMMA nanocomposite particles are mixed into the VAc-VeoVa10 polymer matrix to prepare ZrO_2/PMMA/ VAc-VeoVa10 hybrid coatings. SEM photos demonstrate that the grafting of organic polymers onto inorganic particles can reduce the density mismatch between these two components. So, the hybrid coating with good dispersion stability is obtained. AFM images show that the inorganic-organic nanocomposite particles are homogenously distributed in the VAc-VeoVa10 polymer matrix. Therefore, this two-steps method is very advantageous in introducing inorganic filler particles into organic polymer matrix, especially in a large-scale procedure.

REFERENCES

1 Podsiadlo, P., Kaushik, A.K., Arruda, E.M., Waas, A.M., Shim, B.S., Xu, J., Nandivada, H., Pumplin, B.G., Lahann, J., Ramamoorthy, A., Kotov, N.A., "Ultrastrong and stiff layered polymer nanocomposites", *Science*, **318** (5847), 80−83 (2007).

2 Jeong, S.H., Song, H.C., Lee, W.W., Choi, Y.M., Lee, S.S., Hwan-Ryu, B.Y., "Combined role of well-dispersed aqueous Ag ink and the molecular adhesive layer in inkjet printing the narrow and highly conductive Ag features on a glass substrate", *J. Phys. Chem. C*, **114**, 22277−22283 (2010).

3 Zhang, Y.H., Lv, F.Z., Ke, S.J., Yu, L., Huang, H.T., Chan, H.L.W., "Effect of hollow structure and covalent bonding on the mechanical properties of core-shell silica nanoparticles modified poly(methyl acrylate) composites", *Mater. Chem. Phys.*, **129**, 77−82 (2011).

4 Bokern, S., Getze, J., Agarwal, S., Greiner, A., "Polymer grafted silver and copper nanoparticles with exceptional stability against aggregation by a high yield one-pot synthesis", *Polymer*, **52**, 912−920 (2011).

5 Chigwada, G., Wilkie, C.A., "Synergy between conventional phosphorus fire retardants and organically-modified clays can lead to fire retardancy of styrenics", *Polym. Degrad. Stab.*, **80**, 551−557 (2003).

6 Chigwada, G., Jash, P., Jiang, D.D., Wilkie, C.A., "Synergy between nanocomposite formation and low levels of bromine on fire retardancy in polystyrenes", *Polym. Degrad. Stab.*, **88**, 382−393 (2005).

7 Yutaka, H., Syouzo, I., Sato, T., Yosomiya, R., "Photoconductivity

properties of zinc oxide encapsulated in polymers", *Macromol. Mater. Eng.*, **139**, 49−61 (1986).
8 Caris, C.H.M., Kuijpers, R.P.M., Van Herk, A.M., German, A.L., "Kinetics of (CO) polymerizations at the surface of inorganic submicron particles in emulsion-like systems", *Macromol. Symp.*, **35-36**, 535−548 (1990).
9 Hasegawa, M., Kunio, A., Saito, S., "Effect of surfactant adsorbed on encapsulation of fine inorganic powder with soapless emulsion polymerization", *J. Polym. Sci. A Polym. Chem.*, **25**, 3231−3239 (1987).
10 Agrawal, M., Zafeiropoulos, N.E., Gupta, S., Svetushkina, E., Pionteck, J., Pich, A., Stamm, M., "A novel approach for mixing ZnO nanoparticles into poly(ethyl methacrylate)", *Macromol. Rapid Comm.*, **31**, 405−410 (2010).
11 Schadler, L.S., Kumar, S.K., Benicewicz, B.C., Lewis, S.L., Harton, S.E., "Designed interfaces in polymer nanocomposites: A fundamental viewpoint", *MRS Bull.*, **32**, 335−340 (2007).
12 Pei, X.W., Hao, J.C., Liu, W.M., "Preparation and characterization of carbon nanotubes polymer/Ag hybrid nanocomposites *via* surface RAFT polymerization", *J. Phys. Chem. C*, **111**, 2947−2952 (2007).
13 Wang, B., Wilkes, G.L., "New Ti-PTMO and Zr-PTMO creamer hybrid materials prepared by the sol-gel method: synthesis and characterization", *J. Polym. Sci. A Polym. Chem.*, **29**, 905 (1991).
14 Rehman, H.U., Sarwar, M.I., Ahmad, Z., Krug, H., Schmidt, H., "Synthesis and characterization of novel aramid-zirconium oxide micro-composites", *J. Non-crystal. Solids*, **211**, 105−111 (1997).
15 Di Maggio, R., Fambri, L., Guerriero, A., "Zirconium alkoxides as components of hybrid inorganic-organic macromolecular materials", *Chem. Mater.*, **10**, 1777−1784 (1998).
16 Di Maggio, R., Fambri, L., Mustarelli, P., Campostrini, R., "Physico-chemical characterization of hybrid polymers obtained by 2-hydroxyethyl(methacrylate) and alkoxides of zirconium", *Polymer*, **44**, 7311−7320 (2003).
17 He, W., Guo, Z.G., Pu, Y.K., Yan, L.T., Si, W.J., "Polymer coating on the surface of zirconia nanoparticles by inductively coupled plasma polymerization", *Appl. Phys. Lett.*, **85**, 896−898 (2004).
18 Wang, H.T., Xu, P., Zhong, W., Shen, L., Du, Q.G., "Transparent poly (methyl methacrylate)/silica/zirconia nanoparticles with excellent thermal stabilities", *Polym. Degrad. Stab.*, **87**, 319−327 (2005).
19 Esmaeili, B., Chaouki, J., Dubois, C., "Polymerization compounding on the surface of zirconia nanoparticles", *Macromol. Symp.*, **243**, 268−276 (2006).
20 Sayılkan, F., Asiltürk, M., Burunkaya, E., Arpaç, E., "Hydrothermal synthesis and characterization of nanocrystalline ZrO_2 and surface modification with 2-acetoacetoxyethyl methacrylate", *J. Sol-Gel Sci. Tech.*, **51**, 182−189 (2009).
21 Wang, J., Shi, T.J., Jiang, X.C., "Synthesis and characterization of core-shell ZrO_2/PAAEM/PS nanoparticles", *Nanoscale Res. Lett.*, **4**, 240−246 (2009).
22 Bourgeat-Lami, E., Espiard, Ph., Guyot, A., "Poly(ethyl acrylate) latexes encapsulating nanoparticles of silica: 1. Functionalization and dispersion of silica", *Polymer*, **36**, 4385−4389 (1995).
23 Espiard, Ph., Guyot, A., "Poly(ethyl acrylate) latexes encapsulating nanoparticles of silica: 2. Grafting process onto silica", *Polymer*, **36**, 4391−4395 (1995).
24 Ruehrwein, R.A., Ward, D.W., "Mechanism of clay aggregation by polyelectrolytes", *Soil Sci.*, **73**, 485−492 (1952).
25 Iler, R.K., "Relation of particle size of colloidal silica to the amount of a cationic polymer required for flocculation and surface coverage", *J. Coll. Interf. Sci.*, **37**, 364−373 (1971).
26 Fleer, G.J., Lyklema, J., "Polymer adsorption and its effect on the stability of hydrophobic colloids. Ⅱ. The flocculation process as studied with the silver iodide-polyvinyl alcohol system", *J. Coll. Interf. Sci.*, **46**, 1−12 (1974).
27 Wang, P.C., Chiu, W.Y., Lee, C.F., Young, T.H., "Synthesis of iron oxide/poly(methyl methacrylate) composite latex particles: Nucleation mechanism and morphology", *J. Polym. Sci. A Polym. Chem.*, **42**, 5695−5705 (2004).